C.D.I. Report No. 04-09NP

Methodology to Determine Unsteady Pressure Loading on Components in Reactor Steam Domes

Revision 6

Prepared by:

Continuum Dynamics, Inc.
34 Lexington Avenue
Ewing, NJ 08618

March 2005

Table of Contents

1. Introduction 1
2. Observations and Scaling Considerations 2
3. Methodology Formulation 4
4. Component Models 10
   4.1 Steam Dome 10
   4.2 Main Steam Lines 12
   4.3 Steam Dome/Main Steam Line Junction 13
   4.4 Branch Line Junction 15
   4.5 Control Valves 16
5. Model Assembly 17
6. EPU Loads for Quad Cities Unit 2 (Example Calculation) 21
   6.1 Dryer Peak Pressures 21
   6.2 Dryer Time History 21
   6.3 Validation 21
   6.4 Model Uncertainty 22
7. Sensitivity Analysis 30
   7.1 Sensitivity of Peak Loads to Acoustic Speed in Instrument Lines 30
   7.2 Sensitivity of Dryer Loads to Phasing in Source Region 1 32
8. Conclusions 39
9. References 40
10. Appendix 41

1. Introduction

Estimation of the magnitude of the unsteady pressure loads on components inside a reactor steam dome is complicated by the environment in the dome itself. It is desirable to develop a loads transfer methodology to infer the fluctuating pressure field from existing in-plant measurement transducers, provided that it can be demonstrated that the methodology (algorithm) is robust and accurate. This report documents an algorithm that uses well-established analytical methods to compute the unsteady pressure loading in the steam dome using several simultaneous measurements of pressure in the steam supply system. The model is validated with data taken in the Quad Cities Unit 2 plant by comparing predictions of the fluctuating pressure at a location in the B main steam line with inferred data hoop stress pressure measurements.

2. Observations and Scaling Considerations

Previous analysis of main steam line pressure data [1-3] indicates the presence of discrete frequencies, which suggests that deterministic mechanisms are active in the steam delivery system. Furthermore, these mechanisms are power/flow rate sensitive. Most flow-induced vibration mechanisms that involve unsteady shear layer oscillations scale with dynamic pressure at constant Mach number. For power uprate in boiling water reactor (BWR) plants, system pressures do not change, and increased power is achieved by increasing steam flow velocity in the system. This increase in velocity results in an increase in both the Mach number and dynamic pressure, which scales with the velocity and velocity squared, respectively.

A simple but relevant example illustrates the difficulty in estimating the fluctuating pressures in a complex system. Figure 2-1 illustrates the scaling of the unsteady pressure due to flow over a dead-ended branch line. Data from [4] suggests that the root mean square pressure scales with the dynamic pressure $q = 1/2\ \rho U^2$ at constant Mach number (U/a), where

U is the flow velocity over the branch line

ρ is the fluid density

a is the acoustic speed in the fluid

L is the branch line length

d is the branch line diameter

This scaling can be directly obtained from a scaling analysis. From Figure 2-1, it is apparent that only when $ad/4LU \approx 0.44$ do the pressure fluctuations scale as U^2. For sufficiently low and high velocities, pressure fluctuations disappear.

In a system with many junctions and branch lines of various lengths and diameters, it is clear that a simple "back of the envelope" analysis is not achievable to estimate the unsteady loads as a function of reactor power. For this reason, a methodology is

developed that uses measured in-plant data to infer unsteady loading on the dryer (or any internal component) as a function of reactor power.

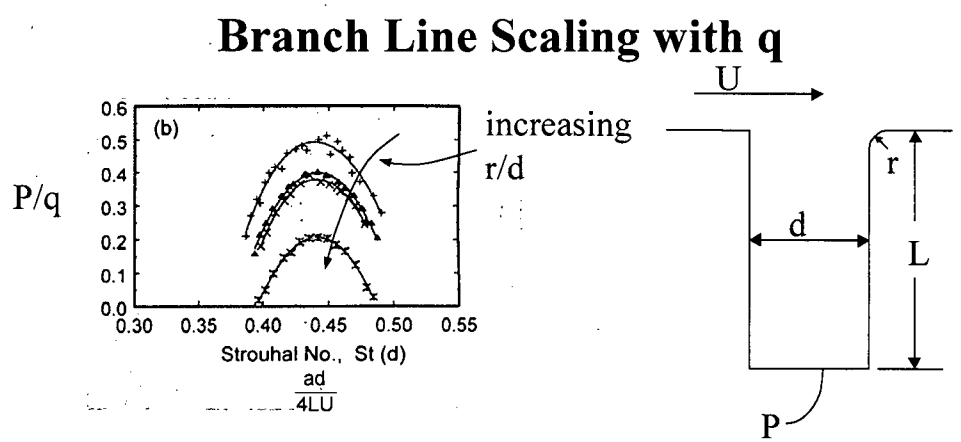

Confirms that oscillation pressure scale with $q=\frac{1}{2}\rho U^2 @ \frac{U}{a}=\text{const.}$

Figure 2-1 Oscillation in a stagnant branch line. (Ref. 4).

3. Methodology Formulation

[[

(3)]]

[[

(3)]]

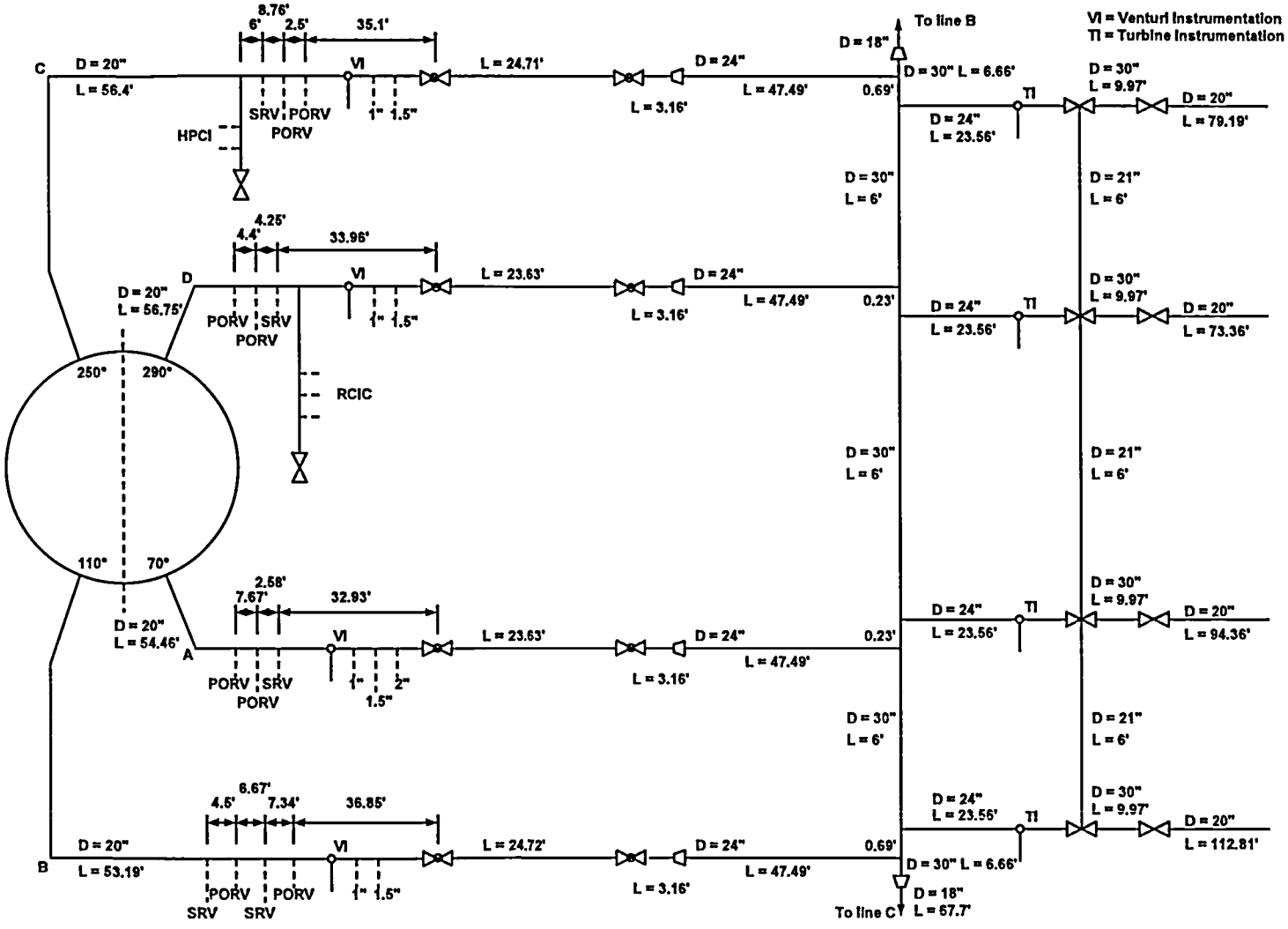

Figure 3-1 Piping geometry used in the acoustic circuit analysis for Quad Cities Unit 2 (QC2).

It is desired to develop an analysis where the pressure field is computed correctly to the order of the Mach number, which is common for hydrodynamic analysis. The hydrodynamic pressure field is typically of the order of Mach number squared. In the steam dome where the Mach number is small, the convective wave equation reduces to the standard wave equation:

$$\frac{1}{a^2}\frac{\partial^2 P}{\partial t^2} - \nabla^2 P = 0$$

In the steam lines where the flow is essentially one-dimensional, the pressure satisfies the following:

$$\frac{1}{a^2}\frac{D^2 P}{Dt^2} - \frac{\partial^2 P}{\partial x^2} = 0$$

where $\frac{D}{Dt} = \frac{\partial}{\partial t} + U\frac{\partial}{\partial x}$, and U is the velocity in the main steam line.

[[

(3)]]

Source region II is well known and exists when a shear flow passes over a dead ended branch line [4, 5]. It is well established that if the velocity over the branch line is $U \approx 0.55\, da/L$, the branch line is excited at the quarter standing acoustic wave in the branch line (also referred to as the first organ pipe mode). Acoustic oscillations exist at a frequency of $a/4L$ and radiate into the flowing system. This mechanism is postulated to occur at the turbine equalizer lines located upstream of the control valves.

[[

(3)]]

The latter measurement is converted to an internal pressure, which is used for model validation. In total, eleven independent measurements are available to deduce the pressure fluctuations in the steam dome for this specific example. However, although sources have been assumed at geometric locations, it is not apparent that analyses of test data would show that some of these sources are in fact negligible.

[[

(3)]]

[[

(3)]]

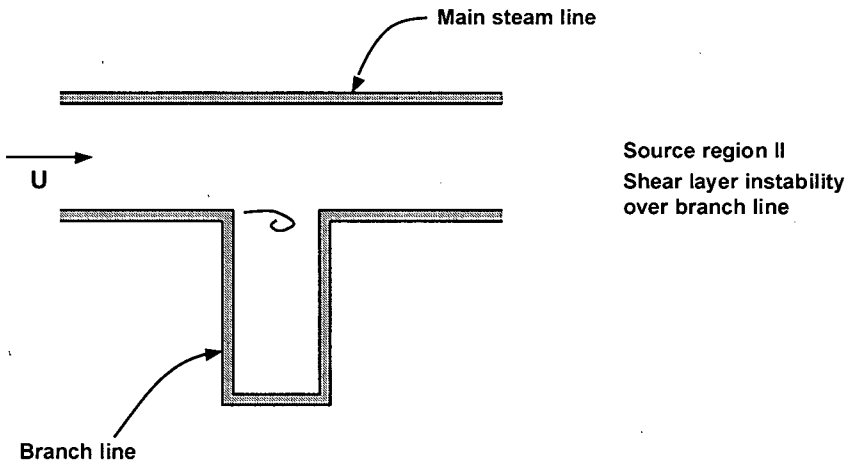

[[

(3)]]

Figure 3-2 Conceptualization of source regions.

4. Component Models

In this section, models used to represent the dynamics of specific component in the steam supply system are described.

4.1 Steam Dome

A cross-section of the steam dome and steam dryer is shown in Figure 4-1 (a schematic top view of the steam dryer is shown in Figure 6.2). Dimensions corresponding the QC2 example, as verified in [6], are also indicated. The unsteady pressure field is determined by periodic solution of the wave equation, since Mach numbers in the steam dome are less than 0.1. Assuming harmonic time dependence, the wave equation reduces to the Helmholtz equation:

$$\nabla^2 P + \frac{\omega^2}{a^2} P = 0$$

where P is pressure, ω is frequency, and a is acoustic speed. The complex three-dimensional geometry of the steam dome is rendered onto a uniformly-spaced rectangular grid with mesh spacing of three inches. The solution for the pressure P is obtained for each grid point within the steam dome.

The Helmholtz equation is solved for incremental frequencies from 0 to 200 Hz, subject to the boundary conditions:

$$\frac{dP}{dn} = 0$$

normal to all solid surfaces (i.e., the steam dome wall and interior and exterior surfaces of the dryer), and:

$$\frac{dP}{dn} = \frac{i\omega}{a} P$$

[[

(3)]]

[[

(3)]]

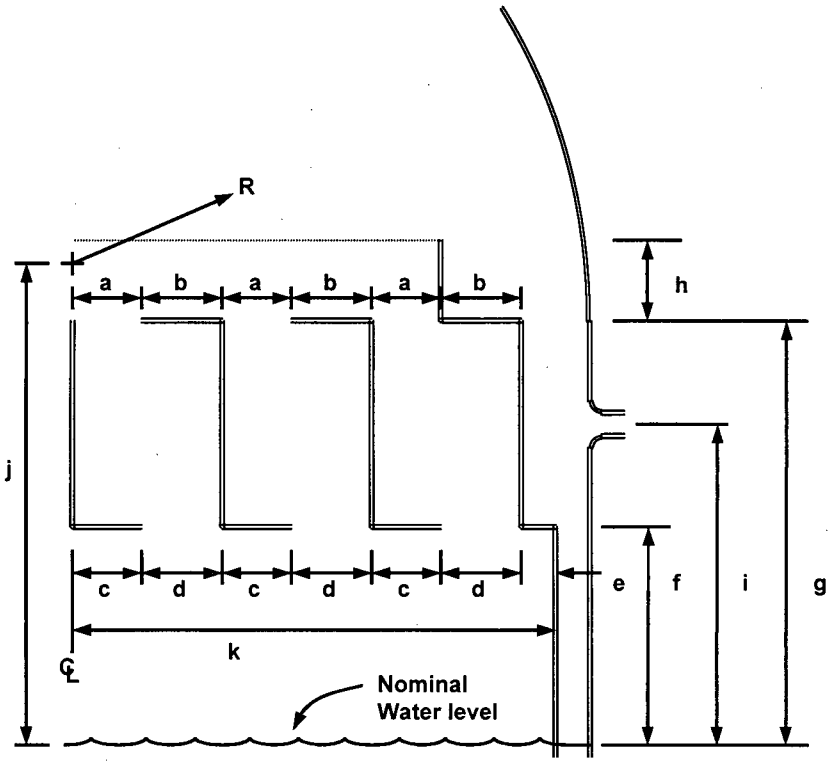

Figure 4-1 **Cross-sectional description of the steam dome and dryer, with the verified QC2 dimensions of a = 6.0 in, b = 28.5 in, c = 15.5 in, d = 19.0 in, e = 16.25 in, f = 75.0 in, g = 137.0 in, h = 23.0 in, i = 88.5 in, j = 166.63 in, k = 120.0 in, and R = 125.5 in.**

[[

Figure 4-2

(3)]]

4.2 Main Steam Lines

The Helmholtz solution within the steam dome is coupled to an acoustic circuit solution in the main steam lines. Pressure fluctuations in single-phase compressible medium, where acoustic wavelengths are long compared to characteristic length scales for the internal components and to transverse dimensions (i.e., directions perpendicular to the primary flow directions), can be determined through application of the acoustic circuit methodology. By restricting the analysis to frequencies below 200 Hz, acoustic

wavelengths are approximately 8 feet in length, which are sufficiently long compared to most components of interest such as branch junctions, etc.

Acoustic circuit analysis separates the main steam lines into elements that are characterized by length L, cross-sectional area A, mean fluid density $\overline{\rho}$, mean flow velocity $\overline{U}$, and mean fluid acoustic speed $\overline{a}$, as illustrated in Figure 4-. Application of acoustic circuit methodology provides solutions for the fluctuating pressure P_n' and velocity u_n' for the nth element of the form:

$$P_n' = \left[A_n e^{ik_{1n}X_n} + B_n e^{ik_{2n}X_n}\right] e^{i\omega t}$$

$$u_n' = -\frac{1}{\overline{\rho a}^2}\left[\frac{\left(\omega + \overline{U}_n k_{1n}\right)}{k_{1n}} A_n e^{ik_{1n}X_n} + \frac{\left(\omega + \overline{U}_n k_{2n}\right)}{k_{2n}} B_n e^{ik_{2n}X_n}\right] e^{i\omega t}$$

where harmonic time dependence of the form $e^{i\omega t}$ has been assumed. The wave numbers k_{1n} and k_{2n} are the two complex roots of the equation:

$$k_n^{\,2} + if_n \frac{\left|\overline{U}_n\right|}{D_n \overline{a}^2}\left(\omega + \overline{U}_n k_n\right) - \frac{1}{\overline{a}^2}\left(\omega + \overline{U}_n k_n\right)^2 = 0$$

where f_n is the pipe friction factor for the nth element, D_n is the hydraulic diameter for the nth element, and $i = \sqrt{-1}$. The complex constants A_n and B_n in the expressions for the fluctuating pressure and velocity above are a function of frequency. These constants are determined by satisfying continuity of pressure and mass conservation at the element junctions.

A similar acoustic circuit analysis is used in the instrument lines to transfer the pressure recorded at the transducer to the main steam line. This analysis is summarized in the Appendix.

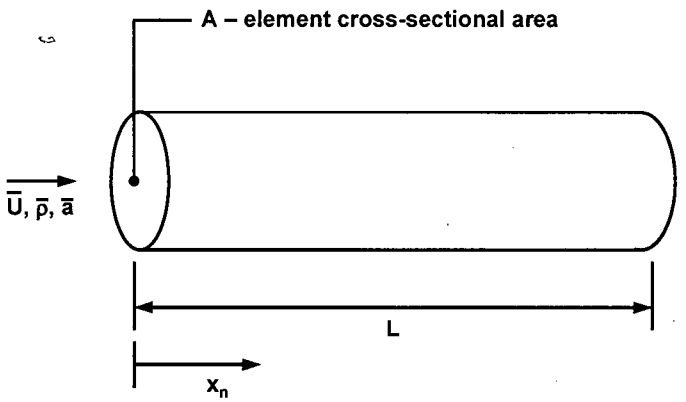

Figure 4-3 Schematic of an element in the acoustic circuit analysis, with length L and cross-sectional area A.

[[

(3)]]

[[

(3)]]

Figure 4-4 Schematic of main steam line inlet region.

4.4 Branch Line Junction

[[

(3)]]

Figure 4-5 Schematic illustrating geometry for branch line analysis.

4.5 Control Valves

Control valves are located before the inlets to the steam turbine and represent the end of the modeled system. Control valves, which are typically open 40%, are modeled with the assumption that downstream acoustic disturbances do not propagate upstream through the valve. This assumption is approximate and becomes more valid as thepressure drop across the valve is increased. [[

[(3)]]

Figure 4-6 Schematic illustrating geometry of control valve analysis.

5. Model Assembly

[[

(3)]]

In-plant data have been obtained as a function of power level on Quad Cities Unit 2. At a given power level, pressure time histories are available at the following locations:

N11A(t) - at the reactor wall at 45° azimuth

N11B(t) - at the reactor wall at 225° azimuth

VA(t) - on the main steam line at venturi A

VB(t) - on the main steam line at venturi B

VC(t) - on the main steam line at venturi C

VD(t) - on the main steam line at venturi D

TA(t) - on the main steam line at turbine instrument line A

TB(t) - on the main steam line at turbine instrument line B

TC(t) - on the main steam line at turbine instrument line C

TD(t) - on the main steam line at turbine instrument line D

SB(t) - hoop stress converted to steam line pressure upstream of the line B ERVs

In total, eleven independent data sets are available. The model in Figure 5-1 **Error! Reference source not found.** has twelve unknown sources, which are:

[[

(3)]]

[[

(3)]]

[[

(3)]]

6. EPU Loads for Quad Cities Unit 2 (Example Calculation)

This section summarizes results from example calculations using the loads transfer methodology. The example uses measured data from the Quad Cities Unit 2 (QC2) steam supply system during extended power uprate (EPU) operation.

6.1 Dryer Peak Pressures

Calculations have been performed using measured EPU data [[

(3)]] Peak pressures and root mean square (RMS) pressure levels are predicted at different dryer locations (node numbers) in Figure 6-1. Physical node locations are shown in Figure 6-2.

[[

(3)]]

6.2 Dryer Time History

The differential pressure and associated power spectral density (PSD) across the cover plate is shown in Figure 6-3. In principle, the model can predict the pressure time history at any location in the steam dome to a resolution of approximately three inches. Examination of the pressure spectrum (PSD) indicates that energy exists at discrete frequencies in the pressure time history.

6.3 Validation

As discussed previously, the strain gage data SB(t) on the B line upstream of the ERVs has not been used in the analysis to provide a separate dataset for model validation. The estimated pressure in the main steam line from strain gage data is shown in Figure

6-4 with its associated PSD. Several calculations were performed varying the bulk acoustic speeds in the instrument lines, and the results of these calculations are shown in Figure 6-5 and Figure 6-6, providing predictions of the pressure at this location for bulk instrument line acoustic speeds of 4600 ft/sec and 4700 ft/sec, respectively. Referring to Figure 6-7 below, these acoustic speeds correspond to bulk instrument line water temperatures of 348.3°F and 326.1°F, respectively.

A comparison of data from Figure 6-4 with model predictions is tabulated below. Comparison of the PSDs shows similar frequency content between measured and predicted pressures.

	Peak Pressure (psid)	**P_{rms} (psid)**
SB	11.44	2.80
Prediction 4600 ft/sec	11.41	2.80
Prediction 4700 ft/sec	11.82	2.79

6.4 Model Uncertainty

The loads transfer methodology to determine the pressure fluctuation magnitudes on the reactor walls or in the main steam lines is undergoing additional validation using a separate full-scale test program. Once this validation program is complete, the measured pressure data will be subject to uncertainty associated with instrumentation measurement accuracy and the assumed acoustic speed in the instrument lines.

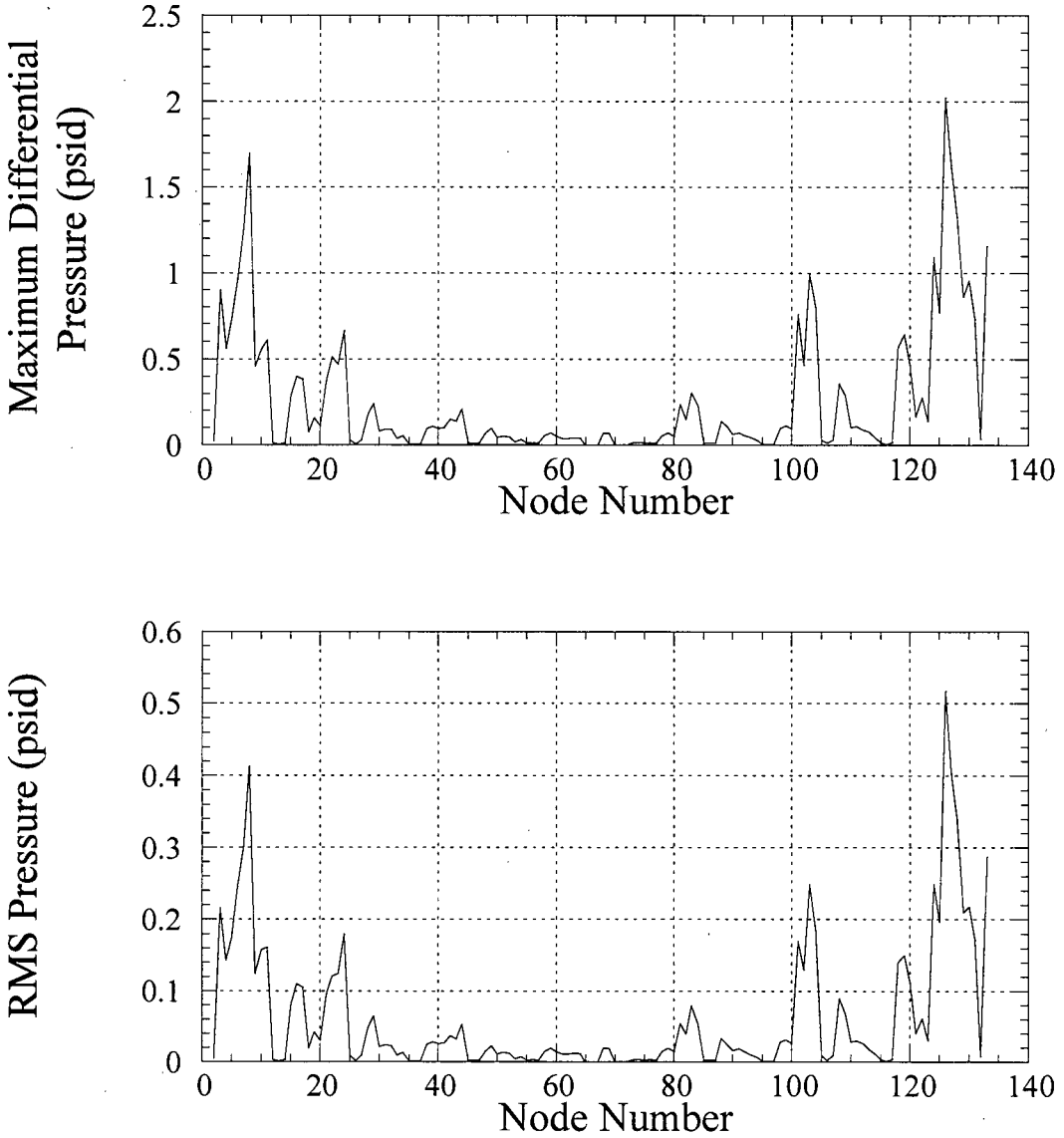

Figure 6-1 EPU loads developed by the current methodology.

TOP VIEW:

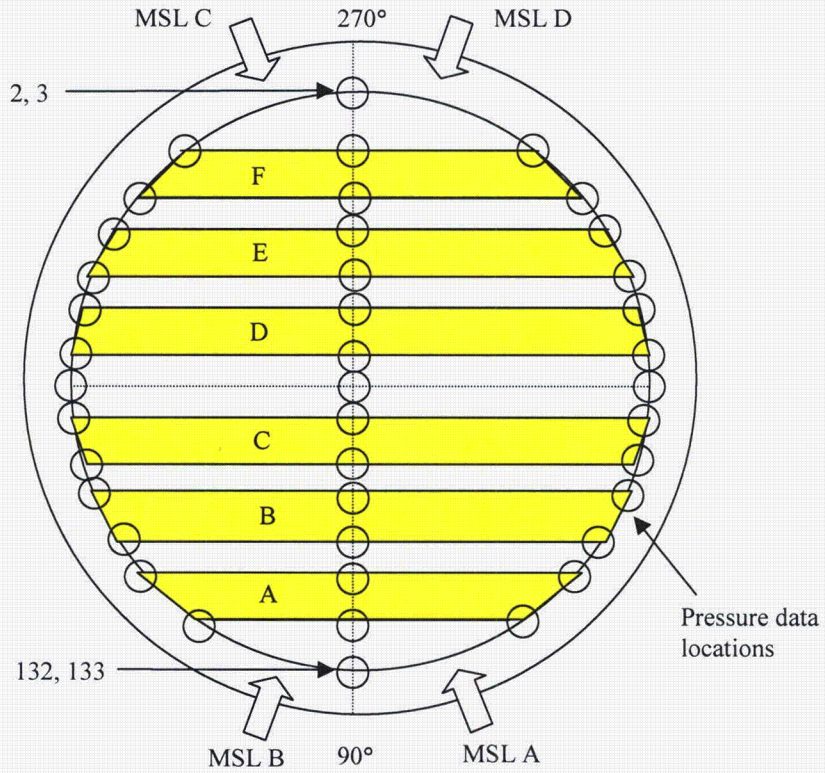

SIDE VIEW:

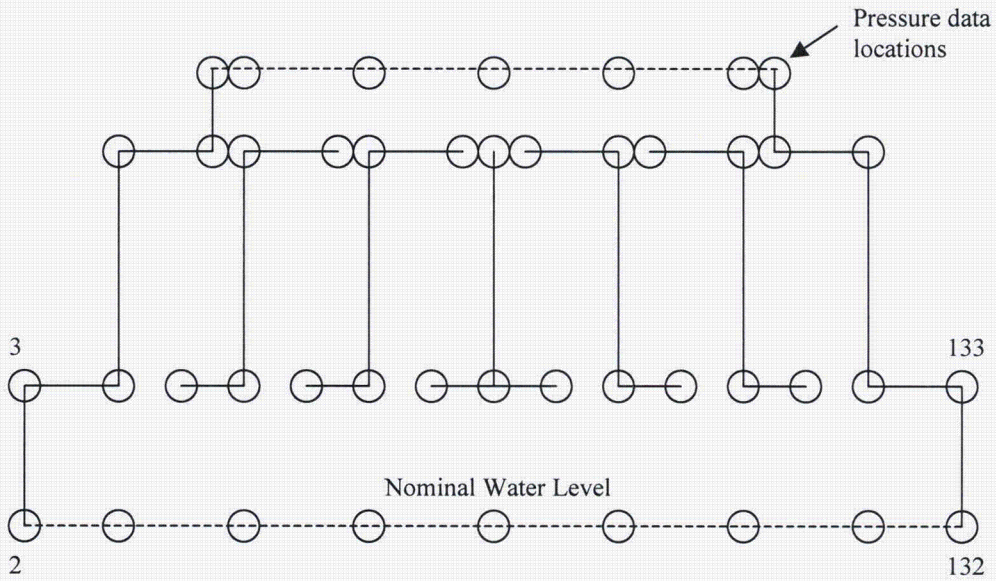

Figure 6-2 Top and side view schematic of pressure node locations on the steam dryer.

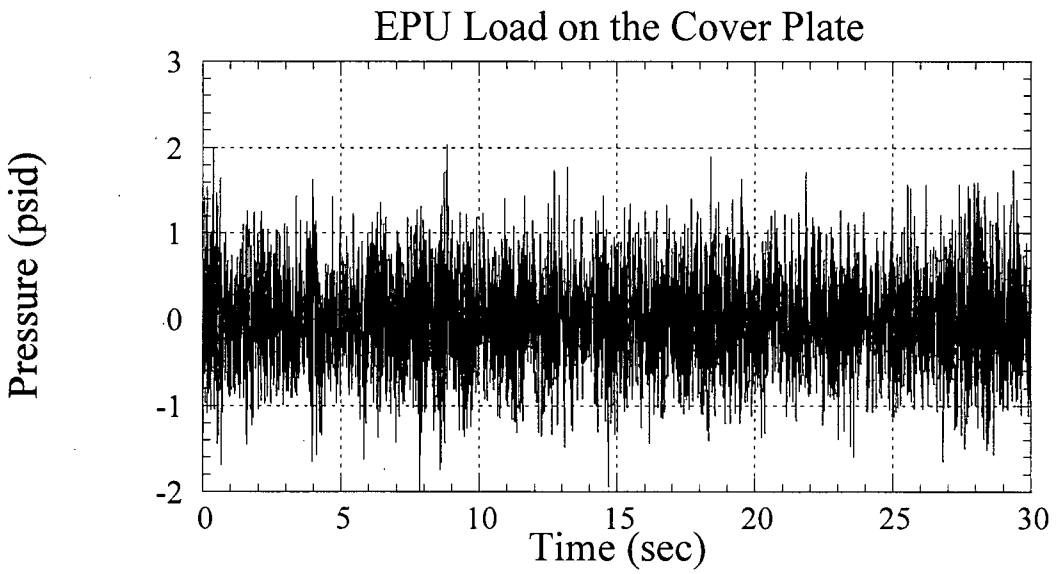

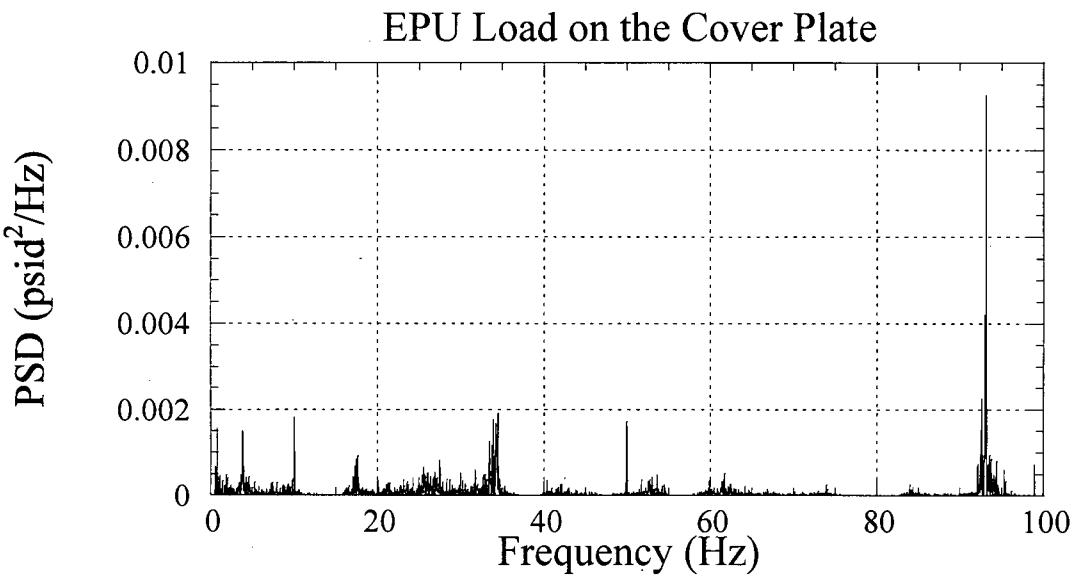

Figure 6-3 **EPU pressure time history and PSD on the cover plate on the A and B main vent side.**

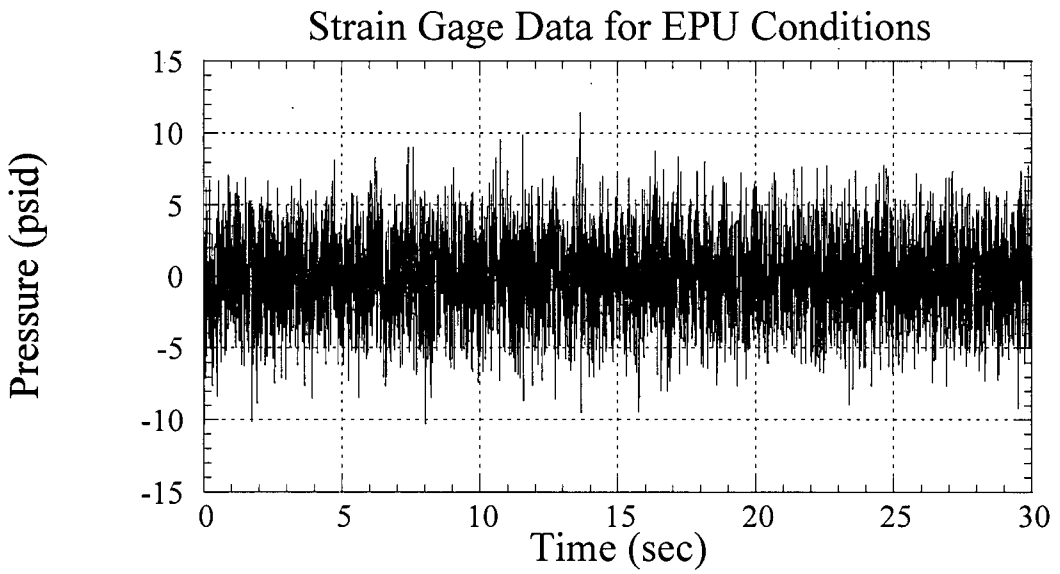

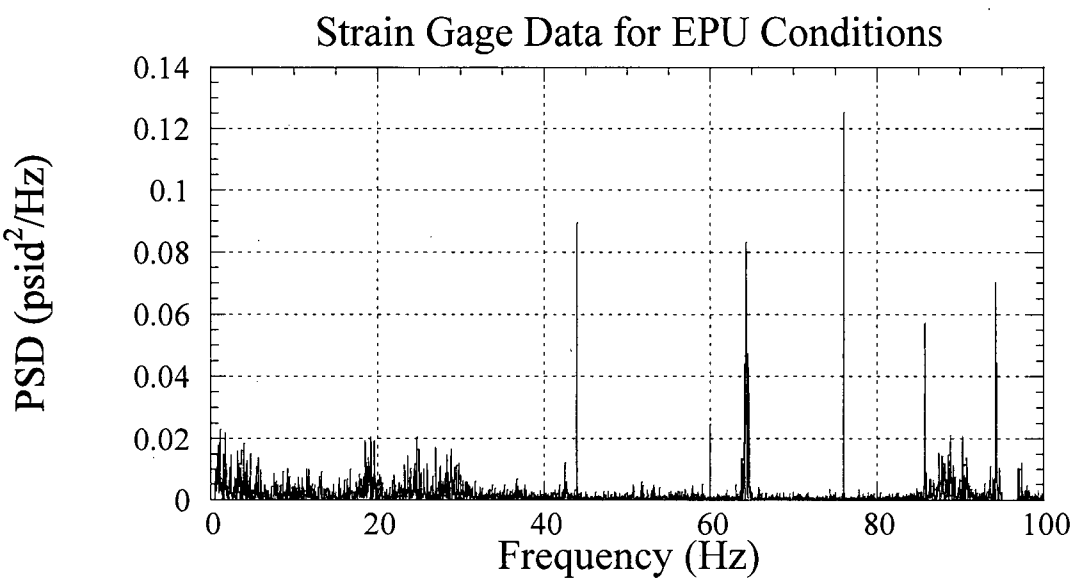

Figure 6-4 EPU pressure time history and PSD derived from strain gage data.

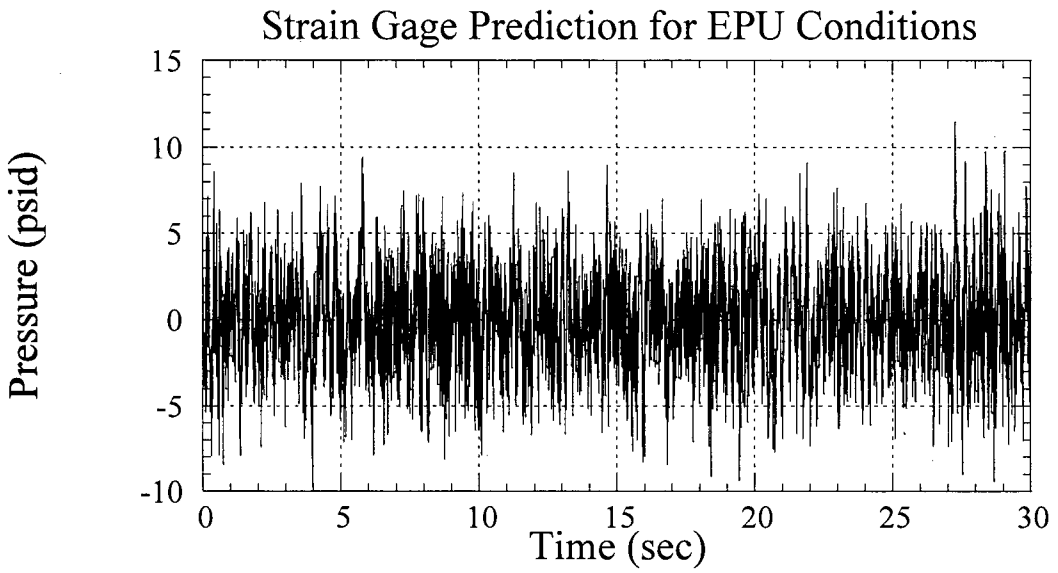

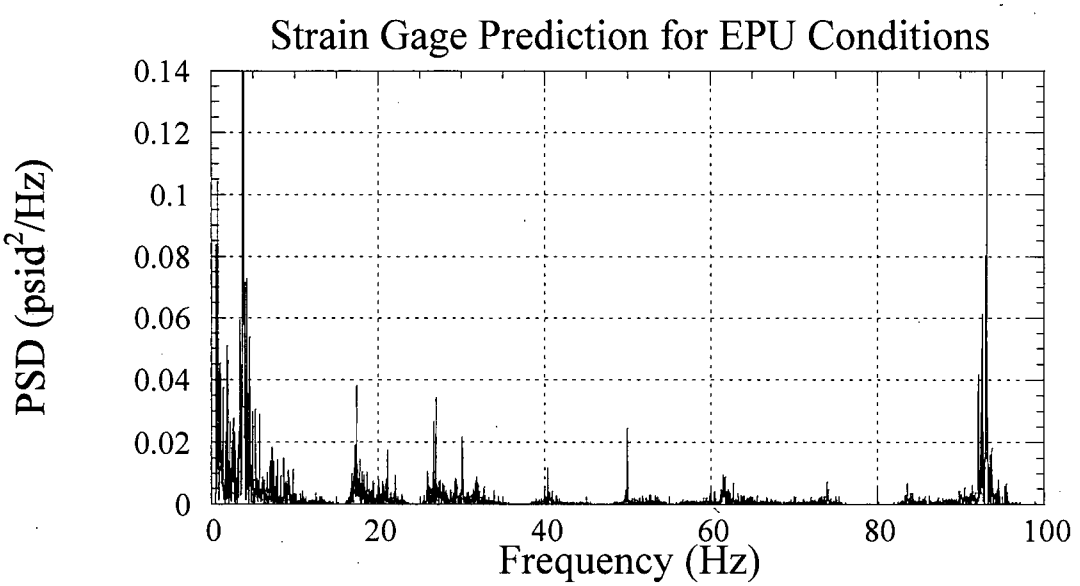

Figure 6-5 **EPU strain gage pressure and PSD predictions with the current methodology, for an acoustic speed of 4600 ft/sec.**

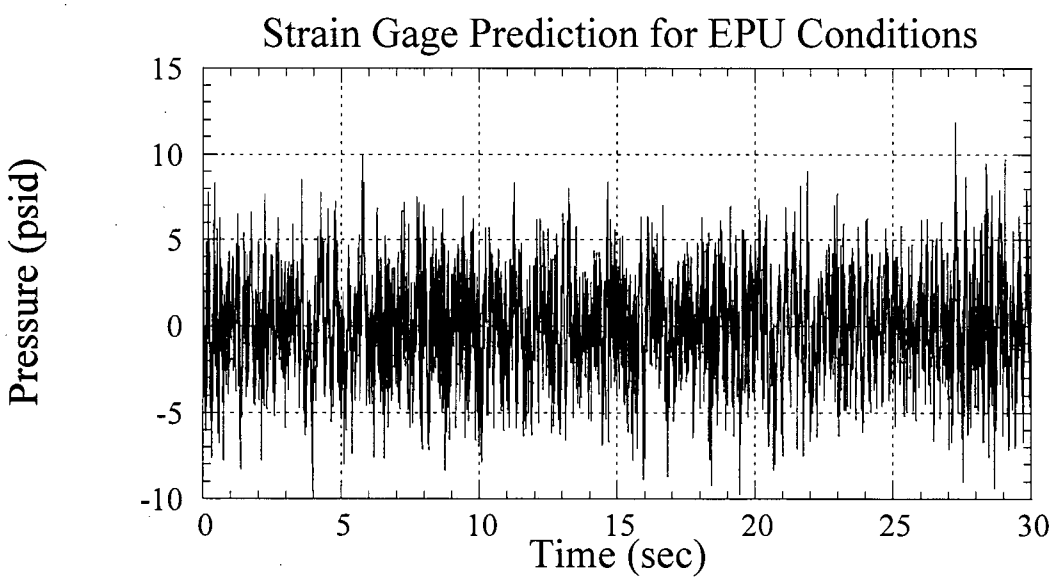

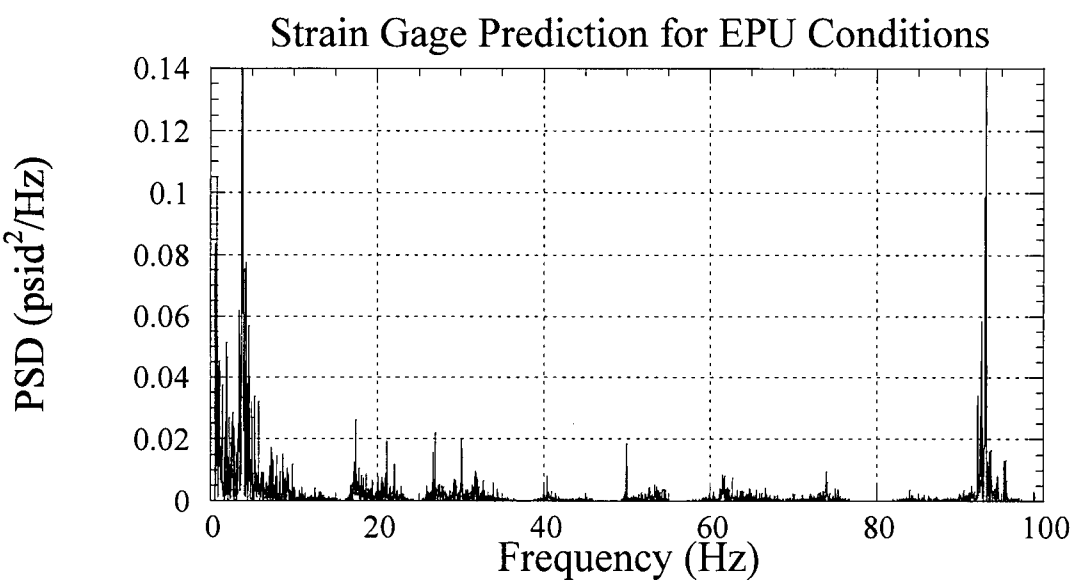

Figure 6-6 **EPU strain gage pressure and PSD predictions with the current methodology, for an acoustic speed of 4700 ft/sec.**

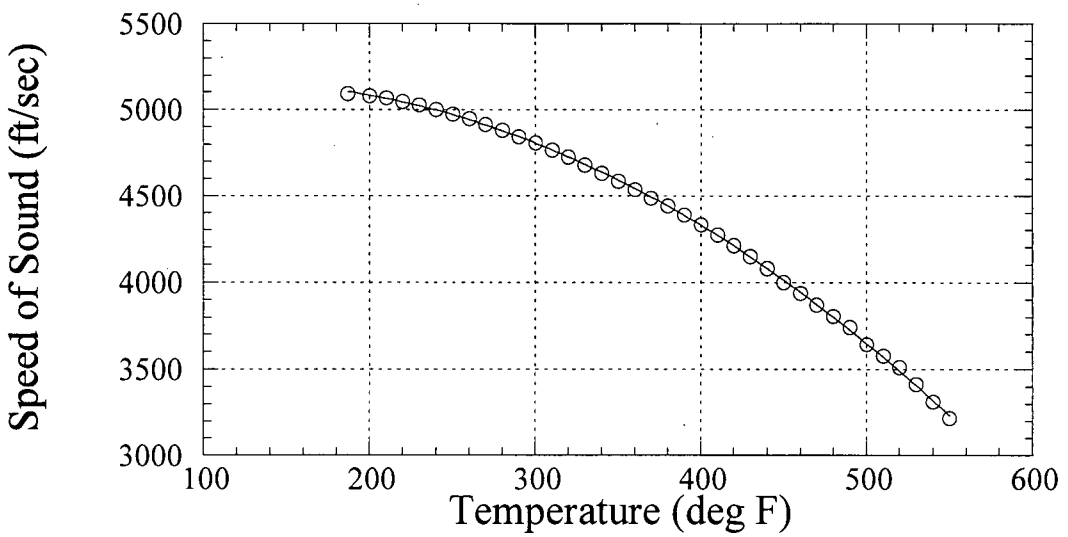

Figure 6-7 Temperature effect on water acoustic speed [7].

7. Sensitivity Analysis

7.1 Sensitivity of Peak Loads to Acoustic Speed in Instrument Lines

The sensitivity of the peak loads on the dryer to the acoustic speed can be determined from the computed dryer loads at two bulk instrument line acoustic speeds. This sensitivity ($\partial P/\partial a$) is shown in Figure 7-1 at an instrument line bulk acoustic speed of 4700 ft/sec. For the predicted load to have an accuracy of 10%, the bulk acoustic speed must be known to within 500 ft/sec.

The sensitivity to instrument measurement error can also be evaluated. This evaluation is required since the pressure fluctuations measured on the reference leg transducers are near the resolution limits of at least one transducer. Calculations were run by increasing the water level transducers by 20%. The changes in the predicted peak pressures on the dryer are shown in Figure 7-2. It is apparent that the dryer load definition uncertainty benefits from water level measurements with improved accuracy.

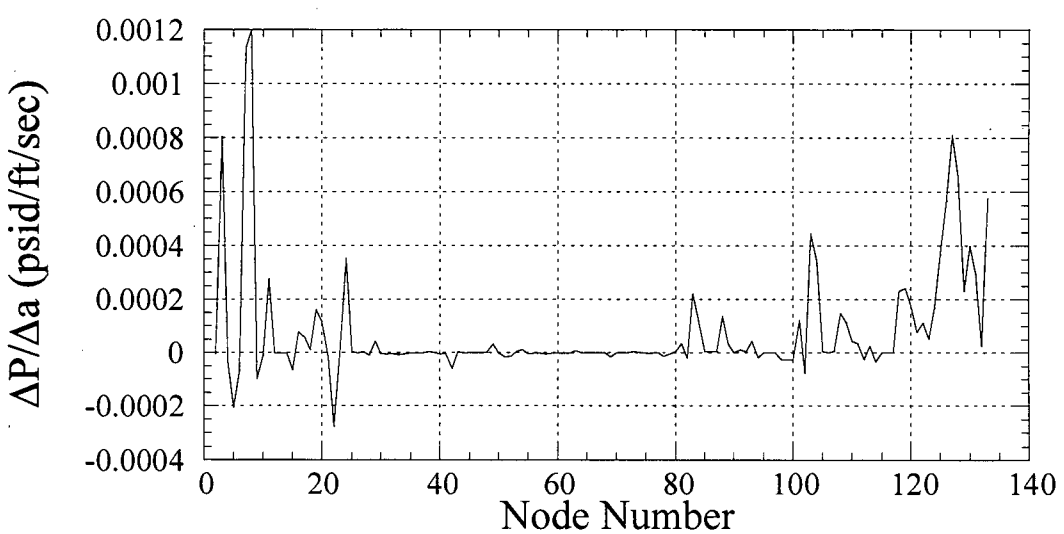

Figure 7-1 Sensitivity of the dryer loads to change in acoustic speed.

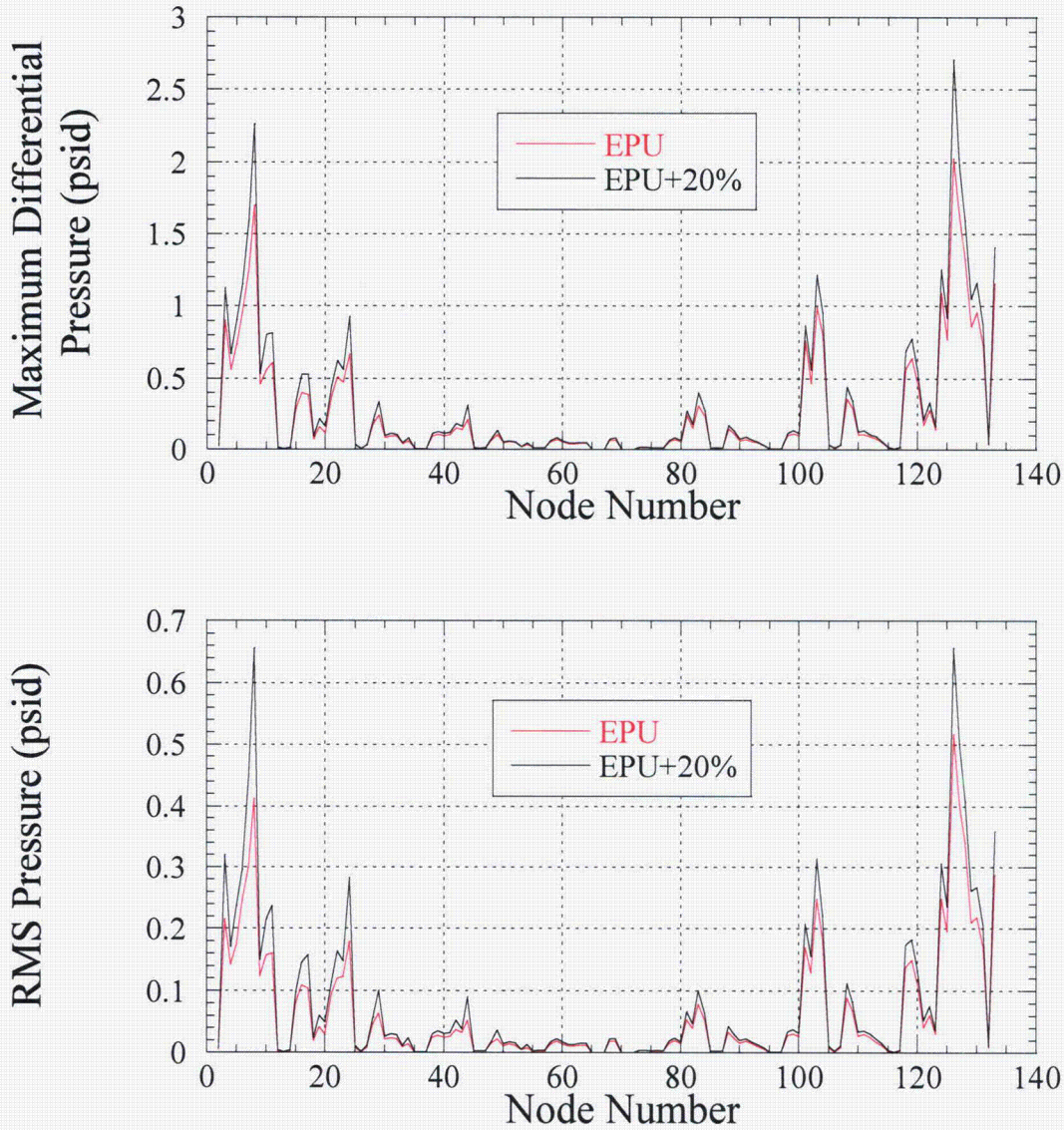

Figure 7-2 **EPU loads developed by the current methodology, with a 20% increase in EPU loads for an acoustic speed of 4700 ft/sec.**

7.2 Sensitivity of Dryer Loads to Phasing in Source Region 1

[[

(3)]]

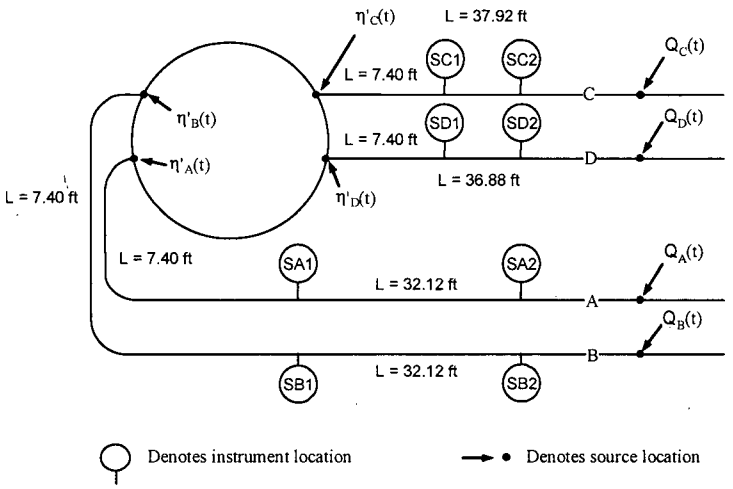

Figure 7.3 Dresden Unit 2 strain gage measurements used for EPU dryer loads.

[[

(3)]]

Figure 7.4 Normalized head loss coefficients of Dresden EPU conditions main steam lines A, B, C and D.

[[

(3)]]

Figure 7.4 (continued)

[[

(3)]]

Figure 7.5 Power Spectral Density function corresponding to the time histories shown in Figure 7.4

[[

[(3)]]

Figure 7.5 (continued)

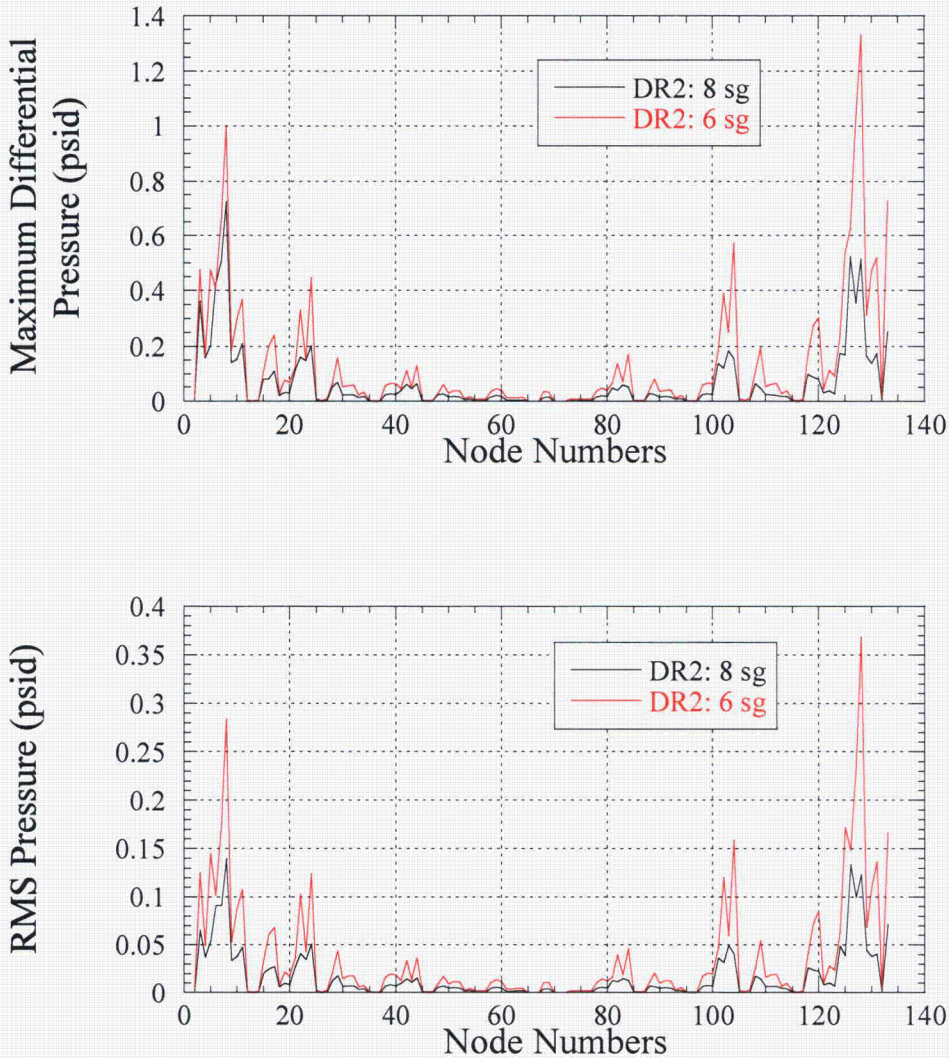

Figure 7.6 Comparison of dryer loads with the assumptions on source region 1 (6 sg) and without assumption (8 sg).

8. Conclusions

A physically-based, loads transfer methodology that can predict loads on reactor components from measurements made external to the reactor steam dome has been developed and validated. The model accounts for acoustic sources at locations along the steam delivery system that are known to provide a region where mean flow energy can be transferred in acoustic pressure oscillations. Accuracy of the model-based loads transfer scheme is most likely limited by in-plant pressure measurement accuracy, and these errors are therefore quantifiable. Following validation of instrument correction algorithms, not discussed in this report, the methodology should reliably provide definition of plant-unique dryer loads.

9. References

1. Continuum Dynamics, Inc., "Hydrodynamic Loads on Quad Cities Unit 1 Steam Dryer," CDI Report No. 03-18, 2003.
2. Continuum Dynamics, Inc., "Hydrodynamic Loads on Dresden Unit 2 Steam Dryer," CDI Report No. 04-01, 2004.
3. Continuum Dynamics, Inc., "Hydrodynamic Loads on Dresden Unit 3 Steam Dryer," CDI Report No. 04-02, 2004.
4. Weaver, D.S. and MacLeod, G.O., "Entrance Port Rounding Effects on Acoustic Resonance in Safety Relief Valves," PVP-Vol. 389, Flow-Induced Vibration, 1999 ASME Pressure Vessels and Piping Conference, Boston, MA, August 1999.
5. Ziada, S., "A Flow Visualization Study of Flow-Acoustic Coupling at the Mouth of a Resonant Side-Branch," PVP Vol. 258, Flow-Induced Vibration and Fluid Structure Interaction, 1993 Pressure Vessels and Piping Conference, Denver, CO, July 1993.
6. Tu, T., "Verification of Dimensions for Quad Cities 1 & 2 and Dresden 2 & 3 Steam Dome and Steam Dryer," GE-NE-0000-0026-6917-11, Rev. 1, 2004.
7. McDade, J. C., D. R. Pardue, A. L. Hedrich and F. Vrataric, "Sound Velocity in Water above 212°F," The Journal of the Acoustical Society of America, 31(10): 1380-1383, 1959.

10. Appendix

[[

(3)]]

[[

(3)]]

[[

[3]]]

Figure A.1. Schematic of instrument line geometry.